

IGNITION OF A TIMBER CEILING: ANALYSING CONVECTIVE AND RADIATIVE HEATING EFFECTS

Joshua Madden¹, Felix Wiesner², David Morisset³, Wenxuan Wu⁴, Ryan Hilditch⁵, Adam Irvine⁶, David Lange⁷

ABSTRACT: Engineered timber buildings require a holistic fire safety strategy that integrates the interaction between the fire-involved structure and the compartment fire dynamics. However, significant research gaps persist, limiting the implementation of a truly holistic design approach. One critical gap is the ignition of an exposed timber ceiling, which can lead to rapid fire spread and abrupt changes in compartment fire conditions, directly impacting the evacuation time. This study investigates the effect of forced convective flow on the ignition delay time of timber under different incident heat fluxes and flow velocities. Tests were conducted in both a normal horizontal (face-up) orientation, and a horizontal inverted (face-down) orientation, representative of an exposed timber ceiling. Results indicate that flow velocity may influence the ignition delay time, particularly in the inverted orientation, which may have implications for predicting the ignition delay time of a mass timber ceiling. Additionally, findings suggest that forced flow may influence whether ignition occurs, introducing stochastic behaviour which is observed under the test conditions used. This study highlights the need for a refined methodology to better characterise ignition behaviour across different mass timber compartment fire scenarios. This improved understanding will support the development of holistic performance-based design for mass timber buildings.

KEYWORDS: Timber, Ignition, Ceiling, Forced-Convection, Radiation

1 – INTRODUCTION

Timber has been a construction material throughout history due to its abundance, versatility, renewability, and high strength-to-weight ratio. Its use however has also been marked by significant fire events, with one of the most notable being the Great Fire of London in 1666, lasting around four days and destroying approximately 13,200 buildings [1]. This disaster accentuated the combustibility of timber and led to changes in building regulations, requiring non-combustible materials to be used, such as stone and brick [2].

Recently, there has been a resurgence of timber use in the form of mass engineered timber, driven by the need for

sustainable infrastructure and efforts to reduce greenhouse gas emissions [3]. Mass timber allows for large uniform cross-sections in comparison to traditional timber, enabling taller timber buildings. However, it remains combustible, and thus poses risks to life, property, and the environment.

This research investigates a critical aspect of ignition of timber ceilings in open-plan compartments. Specifically, the study aims to understand how convective flows impact ignition in ceiling orientations. By investigating this gap, the research seeks to contribute to the development of more comprehensive fire safety strategies for mass timber buildings.

¹ Joshua Madden, School of Civil Engineering, The University of Queensland, Brisbane, Australia, joshua.madden@uq.edu.au

² Felix Wiesner, Department of Wood Science, The University of British Columbia, Vancouver, Canada, felix.wiesner@ubc.ca

³ David Morisset, School of Civil Engineering, The University of Queensland, Brisbane, Australia, d.morisset@uq.edu.au

⁴ Wenxuan Wu, School of Civil Engineering, The University of Queensland, Brisbane, Australia, wenxuan.wu@uq.edu.au

⁵ Ryan Hilditch, Halliwell Fire Research, Brisbane, Australia, ryan.hilditch@halliwellglobal.com

⁶ Adam Irvine, Bloom Fire Consulting, Brisbane, Australia, adam.ervine@bloomfireconsulting.com

⁷ David Lange, School of Civil Engineering, The University of Queensland, Brisbane, Australia, d.lange@uq.edu.au

2 – BACKGROUND

The fire performance of mass timber differs from that of typical steel or concrete structures due to the combustibility of the wood itself. This introduces a feedback loop between the fire and the structural components, as both the movable fuel load and the structural elements contribute to the fire dynamics [4, 5]. This can result in longer burning durations, potentially exceeding the period of adequate compartmentation and structural integrity, increasing the risk of structural collapse and fire spread beyond the compartment of origin [6].

A bespoke fire safety strategy is critical to mass timber buildings to ensure adequate fire performance and occupant life safety [7]. Such a strategy typically includes at least two components: the egress strategy and the building performance, both of which are time dependent [8]. The egress strategy addresses the time required to safely evacuate occupants, while the building performance relates to the structure's ability to withstand fire and maintain compartmentation.

There is a growing body of literature that highlights the limitations of prescriptive design methodologies in evaluating the fire performance of mass timber [9, 10]. These methodologies often do not reflect the actual performance of wood during a fire [11]. Due to its combustible nature, timber requires a fire safety strategy to be developed that explicitly accounts for the combustibility of the structure and the linings, necessitating a shift from prescriptive requirements developed primarily for steel and concrete, to a performance-based design (PBD) methodology. In this approach, the structure and fire are integrated, acknowledging the interactions between the structure and fire dynamics and the impact on the fire safety strategy is assessed [4, 12].

The lack of comprehensive research is a significant barrier to a holistic PBD fire safety strategy for mass timber buildings [4, 12, 13]. At varying scales, existing compartment tests [14-19] have shown that, once a combustible timber ceiling ignites, rapid flame spread across the exposed surface ensues. Despite this, the impact of an exposed ceiling on ignition and subsequent flame spread has received surprisingly limited research attention. More recently, researchers have focused on understanding the phenomena governing ignition within the context of mass timber buildings [20-23].

Exposure to elevated temperatures or radiant heat fluxes, typical in fire conditions, causes timber to undergo physical, chemical, and structural changes [24]. For a solid fuel to ignite, three key criteria must be met: (1) the material must be heated sufficiently to produce

pyrolysates that are mixed with air to create a flammable fuel/oxidiser mixture (2) the fuel/oxidiser mixture must reach a sufficient temperature for piloted or unpiloted ignition to occur; and (3) the heat flux at the surface of the material must be sufficient to maintain this decomposition process for sustained flaming combustion [25].

In charring materials such as timber, pyrolysis yields both combustible pyrolysates and a residual solid-phase char. This char layer, characterised by low thermal conductivity and density, insulates the virgin timber, requiring a higher heat flux at the surface to sustain flaming combustion.

The time to ignition, commonly referred to as the ignition delay time, is a combination of the pyrolysis time, mixing time, and gas induction time [26, 27] as expressed in (1).

$$t_{ig} = t_p + t_m + t_i \quad (1)$$

where t_p the time to reach pyrolysis, t_m the mixing time to create a flammable mixture, and t_i the induction time required to reach an initial sustained ignition.

From basic ignition theory for a semi-infinite thermally thick solid [28], it is commonly assumed that the mixing time and induction time are negligible, and thus the time to ignition is provided in (2).

$$t_{ig} \approx t_p = \frac{\pi}{4} \frac{\overline{k_s} \overline{\rho_s} \overline{C_{p,s}} (T_{ig} - T_0)^2}{a^2 \overline{q_e''^2}} \quad (2)$$

where $\overline{k_s}$ is the global thermal conductivity of the solid (kW/m K), $\overline{\rho_s}$ is the global density of the solid (kg/m³), $\overline{C_{p,s}}$ is the global specific heat of the solid (kJ/kg K), $\overline{\alpha_D}$ is the global thermal diffusivity specific heat of the solid (m²/s), a is the absorptivity of the solid (-), T_{ig} is the ignition temperature (K), T_0 is the ambient temperature (K), $\overline{q_e''}$ is the incident external heat flux (kW/m²), and t_{ig} is the ignition delay time (s).

When comparing the ignition phenomenon of timber in two horizontal orientations—face-up and face-down (i.e., ceiling configuration)—inverting the sample creates a more stratified environment that hinders efficient fuel-air mixing due to buoyancy forces acting on the pyrolysates, providing a fuel rich mixture just below the solid's surface. This results in an increased time to ignition, as experimentally observed at small scales [22, 23, 29].

In the context of a pre-flashover compartment fire, the net heat flux at the ceiling is not only radiative. Significant convective flows of hot gases from the plume and ceiling jet of a movable fuel load fire influence both heat transfer to the solid surface and the mixing time, further affecting the time to ignition. At an intermediate scale, Nothard et. al. [15] postulated that shorter fuel gas residence times

(i.e. the time that fuel vapours stay within the reaction zone) due to convective flows from the moveable fuel load fire, resulted in a delayed ignition of the ceiling.

Nioka et al. [30] undertook one of the first significant studies on stagnation point flow and the ignition delay time. Results demonstrated that increasing flow velocity results in enhanced heat transfer to the surface, but also reduces the residence time, which may counteract the enhanced heat transfer to result in an increased ignition delay time. This finding was also found by Wang and Yang [31]. Therefore, there exists a critical point at which the flow is optimal to result in the shortest ignition delay time.

Atreya and Abu-Zaid [32] were among the first to investigate the impact of convective flows parallel to the surface on the piloted ignition of timber under various radiant heat fluxes. Their study showed that for wood, the ignition delay time increases with an increased air velocity, as a greater mass flux is required to attain a flammable fuel/oxidiser mixture due to the reduced residence time. Results also demonstrated that the minimum external heat flux for ignition is also dependent on air velocity, with an increasing air velocity increasing the minimum heat flux for ignition.

Cordova et al [33] undertook a similar study to that by Atreya and Abu-Zaid [32] but on polymethyl methacrylate (PMMA) rather than wood. Results were generally analogous except for surface temperature correlations. For PMMA, a non-charring material, Cordova et al [33] found that the surface temperature at ignition increased with external heat flux and also external velocity, whilst Atreya and Abu-Zaid [32] found for timber that the surface temperature at ignition increased with a decreasing external heat flux but increased with an increased forced velocity. The difference between the surface temperature phenomena for PMMA [33] and timber [32] was attributed to the charring nature of wood [33], which at heat fluxes decreasing towards the critical heat flux for flaming ignition requires higher surface temperatures to result in ignition due to the low thermal conductivity and low density of the char, effectively insulating the virgin timber and reducing the production of pyrolysates [33].

To the authors' knowledge, no prior research has investigated the impact of convective flows on the ignition of timber in a horizontal inverted (face-down) orientation, highlighting a critical research gap and motivating this study.

3 – METHODOLOGY

The aim of this study is to analyse the impact of combined radiative heat and forced laminar convection (at ambient

temperatures only) on the piloted ignition and autoignition delay times of timber at a normal horizontal (face-up), and an inverted horizontal (face-down) orientation. The following section details the experimental setup, sample preparation and testing conditions.

3.1 EXPERIMENTAL SETUP

This study utilised a bespoke forced convection system designated as the Bushfire Ignition and Spread Test Tunnel (BIST) [34], as illustrated in *Figure 1*. Extensive details can be found in [34] but will be summarised here.

A DC powered air blower with an independent power supply is connected to a serpentine duct, as illustrated in *Figure 1*. It should be noted that for the study herein, the air heating mechanism was not utilised and forced convective flows remained at ambient temperatures.

Within the test section itself, two water-cooled infrared heaters placed side-by-side, as illustrated in *Figure 1*, each with a heating length of 406 mm and a heating width of 43 mm, imposing a heat flux distribution across the exposed surface area of the test specimen (~100 mm x 50 mm). The lamps within the heaters are high-intensity, short-wavelength tungsten emitter with an operating temperature of 2,205 °C and a spectral energy peak wavelength of 1.15 μ m. Each lamp is equipped with an aluminium reflector and a quartz window reflect and protect the reflector and lamp from potential contaminants. These lamps are connected to a controller, allowing the input current to the lamps to be adjusted to reach the desired heat flux at the sample surface.

The wavelengths emitted the spectral emission from the heating source used in this study (similar to that seen in other applications such as the FPA [35]), differ from other radiant sources. This is due to the spectral absorptivity of wood [36, 37] which will result in a different level of absorbed radiation compared to other heating elements such as that in the cone calorimeter.

A 650 mm long, 1.12 mm diameter 80/20 Nickel-Chrome alloy resistance wire was coiled to a diameter of 14 mm, forming a pilot igniter that spans across the width of the test section (~80 mm). This pilot was located immediately downstream of the test specimen, with the underside of the coil positioned approximately 5 mm above the sample surface level, as illustrated in *Figure 1*. A voltage of 24V was passed through the wire by the DC power supply box, with the current automatically adjusted based on the resistance of the wire, enabling it to glow and act as pilot ignition ($P \approx 390$ W).

Testing was conducted in a conventional horizontal orientation (face-up), and in an inverted horizontal

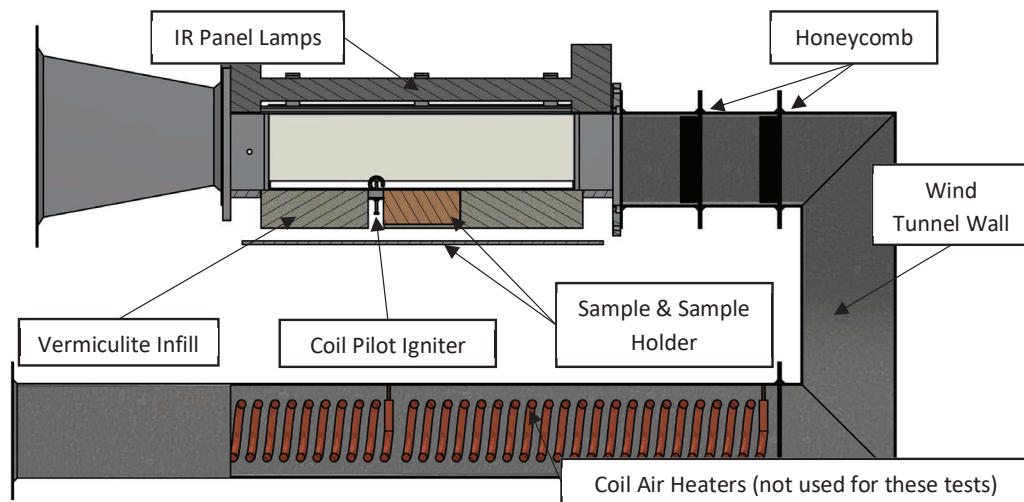


Figure 1. Bushfire Ignition and Spread Test Tunnel- Setup in the Normal Orientation

orientation (face-down) which was enabled by simply flipping the testing apparatus. Heat flux calibrations and mapping was undertaken for both orientations at five locations across the sample surface to determine the spatial distributions under exposure to varying radiant heat fluxes and forced convection conditions. A calibration was performed using a water-cooled Schmidt-Boelter heat flux gauge provided by Hukseflux (SGB01), with a typical sensitivity of $\pm 5\%$ at the maximum operating range of up to 200 kW/m^2 . This gauge measures the incident heat flux (i.e. radiation + convection) at the surface.

Additionally, measurements were taken under exposure to varying heat fluxes and flow conditions in the centre of the sample surface using a water-cooled Gordon gauge with a sapphire window provided by Hukseflux (GG01-250-SW), with a typical sensitivity of $\pm 5\%$ at the maximum operating range of up to 250 kW/m^2 . The addition of the sapphire window ensures that only the radiative heat flux is recorded by the gauge, enabling the calculation of the convective heat flux as the difference between the two gauges.

Where gaps existed between the sample and the opening within the floor of the tunnel ($400 \text{ mm} \times 100 \text{ mm}$), these gaps were sealed with a 45 mm thick vermiculite board, as indicatively illustrated in Figure 1.

3.2 SAMPLE PREPARATION

Samples were cut from the outer lamellae of a three-ply Radiata Pine Cross-Laminated Timber (CLT) slab, with a total thickness of $\sim 125 \text{ mm}$ ($45/35/45 \text{ mm}$). The surface area of the samples was $100 \text{ mm} \times 50 \text{ mm}$, with a depth of 45 mm . This thickness was chosen to ensure that that

the solid could be considered semi-infinite during the experimental duration, allowing neglect of heat losses.

The test samples were taken from the same CLT slab. Prior to testing, the test specimens were stored in a naturally ventilated, non-air-conditioned space for several months. Any samples showing visible natural or manufacturing defects were excluded to avoid impacting the thermal response.

During testing, the moisture constant of other timber samples, from the same CLT slab and stored in the same environment, was tested at least twice weekly using the oven-drying methodology as utilised for previous experiments [23]. The samples had a mean moisture content of 11.21% (Standard Error 0.324%). The tested Normal samples had a mean density of 447.30 kg/m^3 (S.D. 50.27 kg/m^3), whilst the Inverted samples had a mean density of 455.71 kg/m^3 (S.D. 49.2 kg/m^3).

3.3 TESTING CONDITIONS

Prior to testing, the average flow velocity within the wind tunnel was calibrated and recorded both upstream and downstream of the test sample using a hotwire anemometer ($\pm 5\%$ error), taken at an elevation of half the tunnel wall height. Following this, three forced velocities of 0.5 , 1.0 , and 1.5 m/s were selected as boundary conditions for this experimental campaign.

A comparison of the Schmidt-Boelter gauge (radiation + convection) with the Gordon gauge with sapphire window (radiation only) was conducted at the centre of the sample location for 0 , 0.5 , 1.0 , and 1.5 m/s under varying heat fluxes. It was verified that the effect of convective heat transfer was negligible without forced flow from the air blower), and the incident heat flux received at the surface

was predominately radiative. As such, the values derived from the no flow case (i.e. 0 m/s) were used as the boundary conditions for this testing campaign.

With all other boundary conditions constant, a flow velocity of 1.5 m/s results in the highest convective heat transfer for this testing campaign due to a higher Reynolds number. A comparison between the gauges revealed the contribution of the convective heat flux was estimated to be approximately 6-10% of the total net heat flux measured by the gauge under exposure to the same radiative incident heat flux. This does not consider the sensitivities of the respective gauges. However, caution should be exercised, as the gauges are water cooled, resulting in relatively low surface temperatures and subsequent low heat losses.

Prior to the commencement of the formal testing regime, experiments were conducted to determine an approximate minimum heat flux for ignition under exposure to a convective flow. From at least three repeat tests and by bracketing the data, it was found that an approximate minimum heat flux of ignition existed between 25-30 kW/m² for a maximum test time of 900 seconds (i.e. 15 minutes). This is within proximity to the minimum heat flux for ignition found by Atreya and Abu-Zaid [32] under exposure to convective flow at ambient oxygen conditions, when taking into consideration the differences in spectral emissivity and surface absorptivity. Thus, a minimum external heat flux of 30 kW/m² was selected for both orientations. In conclusion external incident radiative heat fluxes of 30, 35, 40, 45 and 50 kW/m² were chosen for this piloted ignition test campaign.

A smaller autoignition campaign was also undertaken as part of this study under external incident radiative heat fluxes of 50 and 55 kW/m² under natural buoyancy (~0 m/s), and forced flows of 0.5, 1.0, and 1.5 m/s.

3.4 PROCEDURES

The test sample was prepared and then placed into the wind tunnel, with all other gaps filled with the vermiculite board. The air blower was then set to the desired voltage and left to stabilise for a period of 60 seconds. During this time, the pilot igniter (if applicable), already fixed in the desired location was switched on to enable the current to flow through, causing it to glow.

Once both the air blower and pilot had stabilised, the lamps were switched on to the desired heat flux. Ignition was considered to occur once flaming was observed for four consecutive seconds, with this time then recorded as the piloted ignition delay time. If no ignition occurred within 600 seconds (10 minutes), the test was stopped

given the diminishing production of pyrolysates and the significant oxidation of the char layer.

A minimum of six repeat tests were undertaken for each heat flux, for each flow condition, in each orientation. This resulted in a total of 182 piloted ignition tests (92 in the Normal and 90 in the Inverted orientations), and 96 autoignition tests (48 per orientation).

4 – RESULTS AND DISCUSSION

The results from piloted ignition are presented in *Figure 2* for both orientations, while *Figure 3* shows the autoignition results. A trendline has been provided for each flow condition by linearising the ignition data and forcing the intercept through the origin, as described in ignition theory [38]. However, a trendline could not be generated for the inverted 1.5m/s autoignition case as only one sample ignited.

For the piloted ignition condition, results demonstrate that an increase in the external heat flux generally leads to a decrease in the ignition delay time, consistent with general ignition theory as per equation (2). A similar trend is observed within the autoignition study, although only two external heat fluxes were tested. These findings align with ignition theory [38] and have been reported by other similar studies [32].

As illustrated within *Figure 2* and *Figure 3*, for the normal orientation, given the significant scatter of the data, there is inconclusive evidence to prove that changes in velocity impact the ignition delay time for piloted ignition. In contrast, for the inverted orientation, results indicate conflicting effects of velocity. Specifically, the ignition delay time increases from a flow velocity of 0.5m/s to 1.0m/s, then decreasing from 1.0m/s to 1.5m/s.

Despite the extensive number of tests undertaken, these results do not appear to align with fundamental fire dynamics observed in previous literature. Studies by Atreya and Abu-Zaid [32] for timber, and Cordova et al [33] for PMMA show an increasing ignition delay time with an increasing flow velocity; whilst others [30, 31] for other materials, suggest that under a forced convective flow, the ignition delay time should initially decrease with increasing flow velocity due to enhanced heat transfer, before increasing again at higher velocities due to the reduced residence time. Results from this study however do not follow either trend, highlighting that ignition is highly system dependent, and can significantly vary depending on the setup used. Thus, non-traditional approaches and methods may be required to understand the impact of velocity on the ignition delay time.

When comparing ignition delay times between the normal and inverted orientations under constant flow velocity and

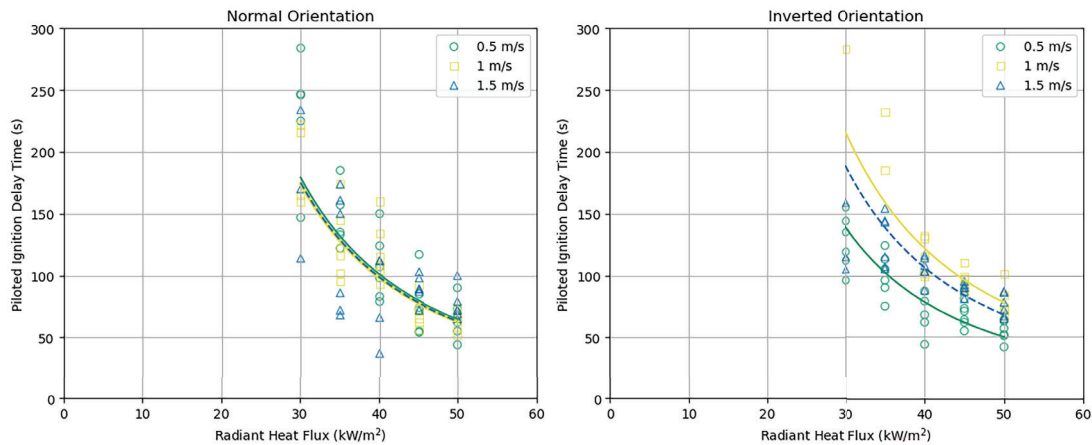


Figure 2. Piloted Ignition Delay Time vs External Radiant Heat Flux for the Normal and Inverted Orientations

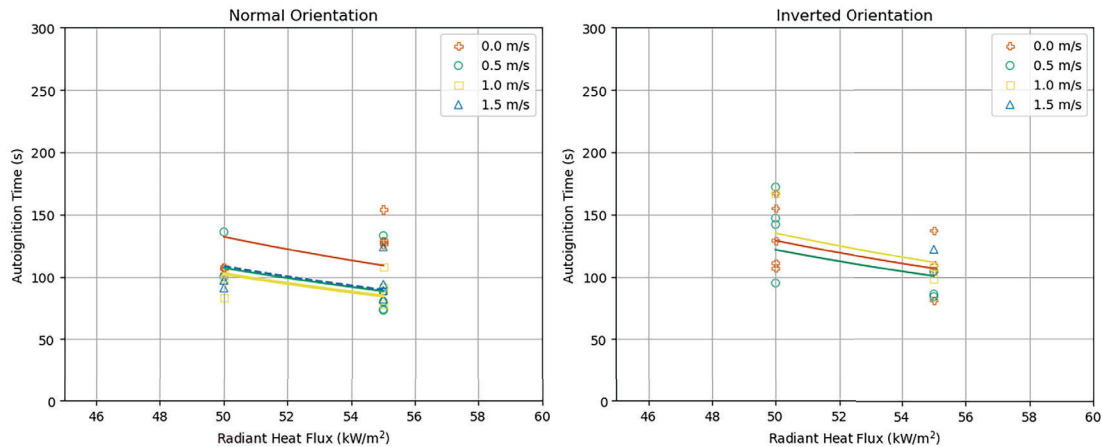


Figure 3. Autoignition Delay Time vs External Radiant Heat Flux for the Normal and Inverted Orientations

external heat flux, there appears to be a general increase in the ignition delay time for the inverted orientation.

However, this difference diminishes at higher heat fluxes and does not always appear to follow this trend. Given the occurrence of non-ignited cases, particularly as the critical heat flux for ignition is approached for both piloted and autoignition, it is difficult to conclude with confidence that inverting the sample consistently increases the ignition delay time.

In fire safety engineering, ignition of timber above critical heat flux is commonly treated as a deterministic event, with ignition being a certainty. However, this study revealed a substantial number of non-ignited cases, suggesting strong variability in whether ignition occurs, and the time at which it does occur, arising from this specific test setup and methodology; particularly as the critical heat flux is approached. This aligns with findings from other research [32, 33] that acknowledge that materials may reach temperatures sufficient to produce

pyrolysates, even though conditions necessary to produce sufficient pyrolysates to support flaming combustion most likely seems to occur.

Table 1 summarises the frequency of non-ignition cases for these test conditions.

Table 1: Summary of ignition occurrence across ignition types and orientations.

Ignition Type	Orientation	Total	No Ignition*
Pilot	Normal	92	10
Pilot	Inverted	90	13
Auto	Normal	48	22
Auto	Inverted	48	28

NB*: No ignition was observed after 600 seconds.

To further explore this, a Lognormal Accelerated Failure Time (AFT) model as per equation (3) [39] was applied to analyse the survival (i.e. non-ignited) probability, treating

ignition delay time as a time-to-event variable and accounting for un-ignited cases (right-censored at 600 s). This approach allows for quantifying the influence of covariates, such as heat flux, flow velocity, and density on both the timing of ignition and the probability of ignition under varying test conditions. Overall, this statistical framework provides a more suitable way of capturing the stochastic variation in time to ignition, which is observed in this study, as per equation (3).

$$S(t) = 1 - \Phi\left(\frac{\log(t) - X\beta}{\sigma}\right) \quad (3)$$

Where $S(t)$ is the probability of surviving (not igniting) beyond time t , $\Phi(-)$ is the standard normal cumulative distribution function, σ is the scale parameter of the lognormal distribution, and $X\beta$ is the linear predictor from the model, calculated as per equation (4).

$$X\beta = \beta_0 + \beta_1 \cdot \text{Velocity} + \beta_2 \cdot \text{Density} \quad (4)$$

Where β_1 and β_2 are coefficients for Velocity and Density, respectively, representing the magnitude of effect on survival probability.

Figure 4, Figure 5, and Figure 6 show the lognormal survival (i.e. no-ignition) curves at velocity levels (0.5, 1.0, and 1.5 m/s) and three heat flux levels (30, 40, and 50 kW/m²) for normal and inverted orientations using piloted ignition. In these plots, density was kept constant to isolate the effects of heat flux and velocity. Key findings from this analysis for this study are follows:

- Across all heat flux levels, increasing the flow velocity generally raises the survival (i.e. non-ignitability), meaning that ignition is less likely (or occurs later). This effect is particularly evident in the inverted configuration, though it is still observable, albeit to a lesser degree, than in the normal orientation.
- As the heat flux increases, overall survival declines (i.e., ignition becomes more likely and occurs sooner). At 50 kW/m², every sample ignites within 300 seconds for all velocities, indicating that heat flux is the dominant factor under these conditions.
- The effect of air velocity on survival appears less significant for the normal orientation, potentially due to a greater variability in sample density, which is a known governing factor in ignition as per equation (2). This variance could overshadow the effect of velocity on ignition timing or occurrence. This interpretation is supported by the model results, where density was marginally significant in the normal configuration ($p=0.12$) but showed no meaningful effect in the inverted configuration

($p=0.82$). Further research should be undertaken to better understand how forced convective flows interact with the fundamental ignition phenomenon, particularly by controlling the density to minimise its potential impact on the ignition delay time.

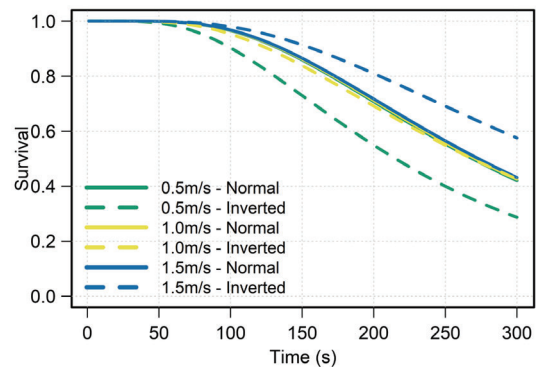


Figure 4. Lognormal survival probability curves at velocity levels (0.5, 1.0, and 1.5 m/s) and heat flux of 30 kW/m² using pilot ignition.

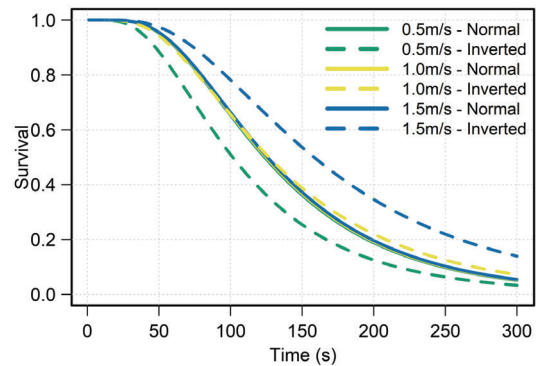


Figure 5. Lognormal survival probability curves at velocity levels (0.5, 1.0, and 1.5 m/s) and heat flux of 40 kW/m² using pilot ignition.

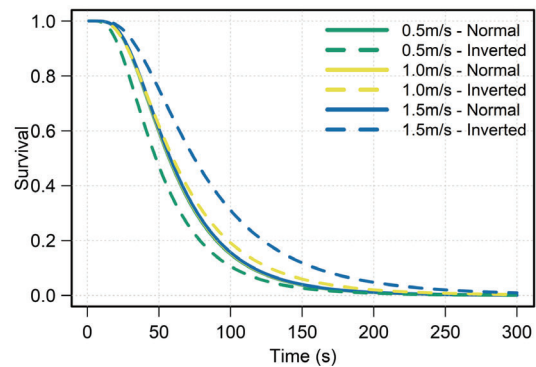


Figure 6. Lognormal survival probability curves at velocity levels (0.5, 1.0, and 1.5 m/s) and heat flux of 50 kW/m² using pilot ignition.

Figure 7 presents lognormal survival (i.e. non-ignited) curves for autoignition at velocity levels (0, 0.5, 1.0, and 1.5 m/s) and high heat flux level (50–55 kW/m²) for the normal and inverted orientations.

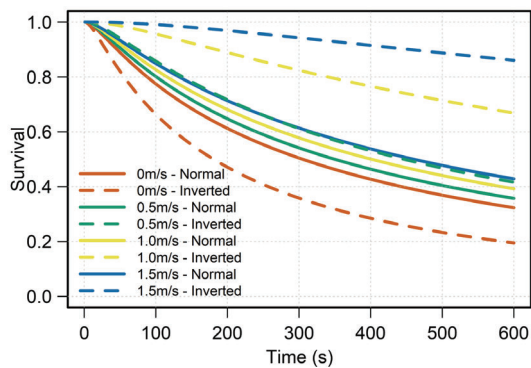


Figure 7. Lognormal survival probability curves at velocity levels (0, 0.5, 1.0, and 1.5 m/s) and high heat flux level (50–55 kW/m²) through auto-ignition.

At these high heat flux conditions, a consistent and comparable pattern was observed: increasing flow velocity leads to higher survival (i.e. non-ignited), delaying or reducing the likelihood of ignition. This effect is more pronounced in the inverted configuration, while it remains more subtle in the normal orientation. The comparatively weaker response in the normal orientation may again be attributed to greater variability in sample density. This is again supported by the model results, where density was not a significant predictor in the inverted configuration ($p=0.98$) but was marginally significant in the normal orientation ($p=0.11$).

As seen above, heat flux became the dominant factor above 50 kW/m²; however, compared to piloted ignition conditions, a higher proportion of un-ignited cases was observed in the auto-ignition setup. This suggests that although the velocity effect persists across configurations, its impact is modulated by ignition mechanism.

It is noted that the above survivability outcomes are specific to this test setup, and do not imply that the ignition of timber as it approaches the critical heat flux is always stochastic. There are several improvements that should be undertaken to refine this study, which could include improvements to the piloted ignition system (i.e. the use of a spark ignitor or pilot flame). Efforts should also be undertaken to control the variance in the density of the timber as from ignition theory, and from the statistical models and literature [40], the density can have an impact on the ignition delay time, and potentially whether ignition will or will not occur for different flow and external heat flux scenarios. Further, a greater range of heat fluxes and flow conditions could be explored to explore whether such a stochastic variation appears at other orientations and in other test conditions.

The AFT approach looking at the survivability (i.e. non-ignited) of timber specimens over the testing period

however offers a new and innovative approach to analysing and predicting ignition, whereby ignition does not need to be treated as deterministic, particularly as the critical heat flux is approached.

5 – CONCLUSION

In this study, 278 bench-scale tests were conducted to investigate the effects of incident heat flux, forced velocity, and orientation on the ignition delay time for piloted and autoignition of radiata pine samples.

As expected, increasing incident heat flux was found to have a decreasing impact on the ignition delay time for all flow velocities and orientations. When comparing orientations, the inverted orientation generally exhibited longer ignition delay times, likely due to the less favourable fuel/oxidiser mixing conditions. This difference diminishes with an increasing heat flux.

The effect of flow velocity on the ignition delay time was less consistent. For the normal orientation, velocity had no clear influence. In contrast, for the inverted orientation, the longest ignition delay times occurred at a flow velocity of 1.0m/s, a result that contradicts existing literature. Given the significant variability in timber density across samples, caution is warranted when interpreting these findings.

Notably, as the critical heat flux for ignition was approached for both the piloted ignition and autoignition cases, ignition was observed to be a stochastic process rather than deterministic given the conditions under which these tests were undertaken. Statistical analysis using an Accelerated Failure Time (AFT) model offers a fresh approach to analysing ignition likelihood of timber which for this study, indicated that at lower heat fluxes, flow velocity influenced the likelihood of ignition over the test durations.

This study challenges the assumption that ignition is always a deterministic event, highlighting that under some boundary conditions, ignition may be stochastic. The introduction of this survivability approach provides new angles to view ignition that could improve the fire-safe design of timber buildings.

Future research should focus on improving the testing methodology, particularly by refining the piloted ignition system and by controlling the density variations for the timber samples. Enhancing these aspects will likely provide more reliable insights into the roles of heat flux, airflow velocity, and timber orientation in ignition behaviour.

ACKNOWLEDGEMENTS

This research was conducted by the **Australian Research Council Research Hub to Advance Timber for Australia's Future Built Environment** (project number IH220100016) funded by the Australian Government. We also acknowledge Sergio Zarate and Hons Wyn for their support.

7 – REFERENCES

[1] I. Smith and M. A. Snow, "Timber: An ancient construction material with a bright future," *The Forestry Chronicle*, vol. 84, no. 4, pp. 504-510, 2008, doi: 10.5558/tfc84504-4.

[2] D. Garrioch, "1666 AND LONDON'S FIRE HISTORY: A RE-EVALUATION," *The Historical Journal*, vol. 59, no. 2, pp. 319-338, 2016, doi: 10.1017/S0018246X15000382.

[3] M. McNamee and B. J. Meacham, "Conceptual Basis for a Sustainable and Fire Resilient Built Environment," *Fire Technology*, 2023/09/20 2023, doi: 10.1007/s10694-023-01490-9.

[4] L. Schmidt, R. Hilditch, A. Ervine, and J. Madden, "Explicit Fire Safety for Modern Mass Timber Structures - From Theory to Practice," in *World Conference on Timber Engineering (WCTE 2023)*, Oslo, Norway, 19-22 June 2023: pp. 1738-1747, doi: <https://doi.org/10.52202/069179-0232>.

[5] F. Wiesner et al., "Large-scale compartment fires to develop a self-extinction design framework for mass timber-Part 2: Results, analysis and design implications," *Fire Safety Journal*, p. 104346, 2025/01/27/ 2025, doi: <https://doi.org/10.1016/j.firesaf.2025.104346>.

[6] A. Law and R. Hadden, "We need to talk about timber: fire safety design in tall buildings," *The Structural Engineer*, vol. 98, no. 3, p. 6, 2020, doi: <https://doi.org/10.56330/XJPS1661>.

[7] D. Lange et al., "A competency framework for fire safety engineering," *Fire Safety Journal*, vol. 127, p. 103511, 2022/01/01/ 2022, doi: <https://doi.org/10.1016/j.firesaf.2021.103511>.

[8] A. Cowlard, A. Bittern, C. Abecassis-Empis, and J. Torero, "Fire Safety Design for Tall Buildings," *Procedia Engineering*, vol. 62, pp. 169-181, 2013/01/01/ 2013, doi: <https://doi.org/10.1016/j.proeng.2013.08.053>.

[9] D. Drysdale, "Steady Burning of Liquids and Solids," in *An Introduction to Fire Dynamics*, 2011, pp. 181-223.

[10] D. Lange, J. Sjöström, J. Schmid, D. Brandon, and J. Hidalgo, "A Comparison of the Conditions in a Fire Resistance Furnace When Testing Combustible and Non-combustible Construction," *Fire Technology*, vol. 56, no. 4, pp. 1621-1654, 2020/07/01 2020, doi: 10.1007/s10694-020-00946-6.

[11] G. Spinardi, "Fire safety regulation: Prescription, performance, and professionalism," *Fire Safety Journal*, vol. 80, pp. 83-88, 2016/02/01/ 2016, doi: <https://doi.org/10.1016/j.firesaf.2015.11.012>.

[12] A. I. Bartlett et al., "Needs For Total Fire Engineering of Mass Timber Buildings," in *2016 World Conference on Timber Engineering (WCTE 2016)*, Vienna, 2016.

[13] J. Madden, R. Hilditch, A. Ervine, L. Schmidt, and D. Lange, "Coupling Fire and Mass Timber Structures: A Challenge Fire Safety Designers Must Address," presented at the *Applications of Structural Fire Engineering (ASFE 24)*, Nanning, China, 25-27 February, 2024.

[14] R. Emberley et al., "Description of small and large-scale cross laminated timber fire tests," *Fire Safety Journal*, vol. 91, pp. 327-335, 2017/07/01/ 2017, doi: <https://doi.org/10.1016/j.firesaf.2017.03.024>.

[15] S. Nothard et al., "Factors influencing the fire dynamics in open-plan compartments with an exposed timber ceiling," *Fire Safety Journal*, vol. 129, p. 103564, 2022, doi: <https://doi.org/10.1016/j.firesaf.2022.103564>.

[16] J. P. Hidalgo et al., "The Malveira fire test: Full-scale demonstration of fire modes in open-plan compartments," *Fire Safety Journal*, vol. 108, p. 102827, 2019/09/01/ 2019, doi: <https://doi.org/10.1016/j.firesaf.2019.102827>.

[17] D. Hopkin et al., "Large-Scale Enclosure Fire Experiments Adopting CLT Slabs with Different Types of Polyurethane Adhesives: Genesis and Preliminary Findings," *Fire*, vol. 5, no. 2, p. 39, 2022. [Online]. Available: <https://www.mdpi.com/2571-6255/5/2/39>.

[18] P. Kotsovinos et al., "Fire dynamics inside a large and open-plan compartment with exposed timber ceiling and columns: CodeRed #01," *Fire and Materials*, vol. 47, no. 4, pp. 542-568, 2023, doi: <https://doi.org/10.1002/fam.3049>.

[19] A. S. Bøe, K. L. Friquin, D. Brandon, A. Steen-Hansen, and I. S. Ertesvåg, "Fire spread in a large compartment with exposed cross-laminated timber and open ventilation conditions: #FRIC-01 – Exposed

- ceiling," *Fire safety journal*, vol. 140, p. 103869, 2023, doi: 10.1016/j.firesaf.2023.103869.
- [20] J. Greer, S. Caponi, R. M. Hadden, and A. Law, "Ignition and Flashover of Reduced Scale Compartments with Timber Ceilings," *Fire Safety Journal*, p. 104167, 2024/04/20/ 2024, doi: <https://doi.org/10.1016/j.firesaf.2024.104167>.
- [21] Z. Qi, H. Hu, and J. Ji, "Investigation on the burning behaviors of the combustible ceiling with the impingement of an incipient fire source," *Energy*, vol. 290, p. 130150, 2024/03/01/ 2024, doi: <https://doi.org/10.1016/j.energy.2023.130150>.
- [22] J. Madden et al., "Burning Behaviour of a Timber Ceiling: A Bench-Scale Investigation," in *SiF 2024 - The 13th International Conference on Structures in Fire*, Coimbra, Portugal, 19 June to 21 June 2024, vol. 1:, pp. 1337 - 1348, doi: https://doi.org/10.30779/cmm_SiF24.
- [23] J. Madden et al., "A method to study ignition of inverted combustible surfaces," *Journal of Physics: Conference Series*, vol. 2885, no. 1, p. 012008, 2024/11/01 2024, doi: 10.1088/1742-6596/2885/1/012008.
- [24] P. Reszka and J. L. Torero, "Fire Behavior of Timber and Lignocellulose," in *Lignocellulosic Fibers and Wood Handbook*, 2016, pp. 553-581.
- [25] V. Babrauskas, *Ignition handbook: principles and applications to fire safety engineering, fire investigation, risk management and forensic science*. Issaquah, WA : Bethesda, Md.: Fire Science Publishers Society of Fire Protection Engineers, 2003.
- [26] A. C. Fernandez-Pello, "Combustion Fundamentals of Fire: The Solid Phase," in *Chapter*, vol. 2, G. Cox Ed. London: Academic Press Limited, 1995, pp. 31-100.
- [27] R. T. Long Jr, J. L. Torero, J. G. Quintiere, and A. C. Fernandez-Pello, "Scale and Transport Considerations on Piloted Ignition of PMMA," in *Fire Safety Science*, 2000 2000, vol. 6, pp. 567-578, doi: 10.3801/IAFSS.FSS.6-567.
- [28] D. Drysdale, "Ignition: The Initiation of Flaming Combustion," in *An Introduction to Fire Dynamics*, 2011, pp. 225-275.
- [29] T. J. Shields, G. W. Silcock, and J. J. Murray, "The effects of geometry and ignition mode on ignition times obtained using a cone calorimeter and ISO ignitability apparatus," *Fire and Materials*, vol. 17, no. 1, pp. 25-32, 1993, doi: <https://doi.org/10.1002/fam.810170105>.
- [30] T. Niioka, M. Takahashi, and M. Izumikawa, "Gas-phase ignition of a solid fuel in a hot stagnation-point flow," *Symposium (International) on Combustion*, vol. 18, no. 1, pp. 741-747, 1981/01/01/ 1981, doi: [https://doi.org/10.1016/S0082-0784\(81\)80078-1](https://doi.org/10.1016/S0082-0784(81)80078-1).
- [31] G.-G. Wang and J.-T. Yang, "Convective thermal ignition of an individual polymethylmethacrylate particle," *Journal of Thermophysics and Heat Transfer*, vol. 6, no. 2, pp. 333-340, 1992, doi: 10.2514/3.364.
- [32] A. Atreya and M. Abu-zaid, "Effect Of Environmental Variables On Piloted Ignition," *Fire Safety Science*, vol. 3, pp. 177-186, 1991, doi: 10.3801/IAFSS.FSS.3-177.
- [33] J. L. Cordova, D. C. Walther, J. L. Torero, and A. C. Fernandez-Pello, "Oxidizer Flow Effects on the Flammability of Solid Combustibles," *Combustion Science and Technology*, vol. 164, no. 1, pp. 253-278, 2001/03/01 2001, doi: 10.1080/00102200108952172.
- [34] S. A. Zarate Orrego, "Contribution of convection and radiation at the preheating stage during fire spread in fuel beds," PhD, School of Civil Engineering, The University of Queensland, 2023.
- [35] ASTM E2058 - 19, A. S. f. T. a. Materials, West Conshohocken, PA, 2019 2019.
- [36] M. Chaos, "Spectral Aspects of Bench-Scale Flammability Testing: Application to Hardwood Pyrolysis," *Fire safety science*, vol. 11, pp. 165-178, 2014, doi: 10.3801/iafss.fss.11-165.
- [37] P. Girods, N. Bal, H. Biteau, G. Rein, and J. Torero, "Comparison of Pyrolysis Behavior Results between the Cone Calorimeter and the Fire Propagation Apparatus Heat Sources," vol. 10, 2011, doi: 10.3801/IAFSS.FSS.10-889.
- [38] J. Torero, "SFPE Handbook of Fire Protection Engineering." New York, NY: Springer New York, 2016, pp. 633-661.
- [39] P. Lambert, D. Collett, A. Kimber, and R. Johnson, "Parametric accelerated failure time models with random effects and an application to kidney transplant survival," *Statistics in Medicine*, vol. 23, no. 20, pp. 3177-3192, 2004, doi: <https://doi.org/10.1002/sim.1876>.
- [40] F. Wiesner, B. McGiveron, T. Liu, J. P. Hidalgo, and J. J. Morrell, "Bushfire performance of native Australian wood species," *Fire Safety Journal*, vol. 140, p. 103884, 2023/10/01/ 2023, doi: <https://doi.org/10.1016/j.firesaf.2023.103884>.